Observation of $B^0 \to p\bar{p}K^{*0}$ with a Large K^{*0} Polarization

J.-H. Chen,[25] M.-Z. Wang,[25] I. Adachi,[8] H. Aihara,[42] K. Arinstein,[1] V. Aulchenko,[1] T. Aushev,[17,12] A. M. Bakich,[37] V. Balagura,[12] E. Barberio,[20] A. Bay,[17] I. Bedny,[1] K. Belous,[11] U. Bitenc,[13] A. Bondar,[1] A. Bozek,[26] M. Bračko,[19,13] T. E. Browder,[7] M.-C. Chang,[3] Y. Chao,[25] A. Chen,[23] K.-F. Chen,[25] W. T. Chen,[23] B. G. Cheon,[6] R. Chistov,[12] I.-S. Cho,[47] S.-K. Choi,[5] Y. Choi,[36] J. Dalseno,[20] M. Dash,[46] A. Drutskoy,[2] S. Eidelman,[1] B. Golob,[18,13] H. Ha,[15] J. Haba,[8] T. Hara,[31] K. Hayasaka,[21] H. Hayashii,[22] M. Hazumi,[8] D. Heffernan,[31] Y. Hoshi,[40] W.-S. Hou,[25] Y. B. Hsiung,[25] H. J. Hyun,[16] K. Inami,[21] A. Ishikawa,[33] H. Ishino,[43] R. Itoh,[8] M. Iwasaki,[42] N. J. Joshi,[38] D. H. Kah,[16] H. Kaji,[21] P. Kapusta,[26] N. Katayama,[8] T. Kawasaki,[28] H. Kichimi,[8] H. J. Kim,[16] S. K. Kim,[35] Y. J. Kim,[4] K. Kinoshita,[2] P. Krokovny,[8] R. Kumar,[32] C. C. Kuo,[23] Y.-J. Kwon,[47] J. S. Lee,[36] M. J. Lee,[35] S. E. Lee,[35] T. Lesiak,[26] J. Li,[7] A. Limosani,[20] C. Liu,[34] D. Liventsev,[12] F. Mandl,[10] A. Matyja,[26] S. McOnie,[37] T. Medvedeva,[12] W. Mitaroff,[10] H. Miyake,[31] H. Miyata,[28] Y. Miyazaki,[21] R. Mizuk,[12] E. Nakano,[30] M. Nakao,[8] H. Nakazawa,[23] Z. Natkaniec,[26] S. Nishida,[8] O. Nitoh,[45] S. Ogawa,[39] T. Ohshima,[21] S. Okuno,[14] S. L. Olsen,[7,9] H. Ozaki,[8] P. Pakhlov,[12] G. Pakhlova,[12] H. Palka,[26] C. W. Park,[36] H. Park,[16] L. S. Peak,[37] R. Pestotnik,[13] L. E. Piilonen,[46] M. Rozanska,[26] H. Sahoo,[7] Y. Sakai,[8] O. Schneider,[17] K. Senyo,[21] M. E. Sevior,[20] M. Shapkin,[11] C. P. Shen,[9] H. Shibuya,[39] J.-G. Shiu,[25] J. B. Singh,[32] A. Somov,[2] S. Stanič,[29] M. Starič,[13] T. Sumiyoshi,[44] F. Takasaki,[8] M. Tanaka,[8] G. N. Taylor,[20] Y. Teramoto,[30] I. Tikhomirov,[12] K. Trabelsi,[8] S. Uehara,[8] K. Ueno,[25] T. Uglov,[12] Y. Unno,[6] S. Uno,[8] P. Urquijo,[20] Y. Usov,[1] G. Varner,[7] K. Vervink,[17] S. Villa,[17] A. Vinokurova,[1] C. C. Wang,[25] C. H. Wang,[24] P. Wang,[9] X. L. Wang,[9] Y. Watanabe,[14] R. Wedd,[20] E. Won,[15] H. Yamamoto,[41] Y. Yamashita,[27] C. C. Zhang,[9] Z. P. Zhang,[34] V. Zhulanov,[1] and A. Zupanc[13]

(Belle Collaboration)

[1]*Budker Institute of Nuclear Physics, Novosibirsk*
[2]*University of Cincinnati, Cincinnati, Ohio 45221*
[3]*Department of Physics, Fu Jen Catholic University, Taipei*
[4]*The Graduate University for Advanced Studies, Hayama*
[5]*Gyeongsang National University, Chinju*
[6]*Hanyang University, Seoul*
[7]*University of Hawaii, Honolulu, Hawaii 96822*
[8]*High Energy Accelerator Research Organization (KEK), Tsukuba*
[9]*Institute of High Energy Physics, Chinese Academy of Sciences, Beijing*
[10]*Institute of High Energy Physics, Vienna*
[11]*Institute of High Energy Physics, Protvino*
[12]*Institute for Theoretical and Experimental Physics, Moscow*
[13]*J. Stefan Institute, Ljubljana*
[14]*Kanagawa University, Yokohama*
[15]*Korea University, Seoul*
[16]*Kyungpook National University, Taegu*
[17]*École Polytechnique Fédérale de Lausanne (EPFL), Lausanne*
[18]*Faculty of Mathematics and Physics, University of Ljubljana, Ljubljana*
[19]*University of Maribor, Maribor*
[20]*University of Melbourne, School of Physics, Victoria 3010*
[21]*Nagoya University, Nagoya*
[22]*Nara Women's University, Nara*
[23]*National Central University, Chung-li*
[24]*National United University, Miao Li*
[25]*Department of Physics, National Taiwan University, Taipei*
[26]*H. Niewodniczanski Institute of Nuclear Physics, Krakow*
[27]*Nippon Dental University, Niigata*
[28]*Niigata University, Niigata*
[29]*University of Nova Gorica, Nova Gorica*
[30]*Osaka City University, Osaka*
[31]*Osaka University, Osaka*
[32]*Panjab University, Chandigarh*
[33]*Saga University, Saga*
[34]*University of Science and Technology of China, Hefei*

[35]*Seoul National University, Seoul*
[36]*Sungkyunkwan University, Suwon*
[37]*University of Sydney, Sydney, New South Wales*
[38]*Tata Institute of Fundamental Research, Mumbai*
[39]*Toho University, Funabashi*
[40]*Tohoku Gakuin University, Tagajo*
[41]*Tohoku University, Sendai*
[42]*Department of Physics, University of Tokyo, Tokyo*
[43]*Tokyo Institute of Technology, Tokyo*
[44]*Tokyo Metropolitan University, Tokyo*
[45]*Tokyo University of Agriculture and Technology, Tokyo*
[46]*Virginia Polytechnic Institute and State University, Blacksburg, Virginia 24061*
[47]*Yonsei University, Seoul*

Using a 492 fb^{-1} data sample collected near the $\Upsilon(4S)$ resonance with the Belle detector at the KEKB asymmetric-energy e^+e^- collider, we observe the decay $B^0 \to p\bar{p}K^{*0}$ with a branching fraction of $(1.18^{+0.29}_{-0.25}(\text{stat}) \pm 0.11(\text{syst})) \times 10^{-6}$. We study the decay dynamics of $B^0 \to p\bar{p}K^{*0}$ and compare with $B^+ \to p\bar{p}K^{*+}$. The K^{*0} meson is found to be almost 100% polarized (with a fraction of $(101 \pm 13 \pm 3)\%$ in the helicity zero state), while the K^{*+} meson has a $(32 \pm 17 \pm 9)\%$ fraction in the helicity zero state. The direct CP asymmetries for $B^0 \to p\bar{p}K^{*0}$ and $B^+ \to p\bar{p}K^{*+}$ are measured to be $-0.08 \pm 0.20 \pm 0.02$ and $-0.01 \pm 0.19 \pm 0.02$, respectively. In addition, we report improved measurements of the branching fractions $\mathcal{B}(B^+ \to p\bar{p}K^{*+}) = (3.38^{+0.73}_{-0.60} \pm 0.39) \times 10^{-6}$ and $\mathcal{B}(B^0 \to p\bar{p}K^0) = (2.51^{+0.35}_{-0.29} \pm 0.21) \times 10^{-6}$, which supersede our previous measurements.

After the first observation of the charmless baryonic B meson decay, $B^+ \to p\bar{p}K^+$ [1,2], many three-body charmless baryonic decays were found [3–6]. One important and intriguing feature of these decays is that the baryon-antibaryon mass distributions all peak near threshold. However, the *BABAR* collaboration recently reported evidence of the decay $B^0 \to p\bar{p}K^{*0}$ but could not establish either the presence or absence of such a threshold enhancement [7]. On the theoretical side, it is generally believed that the $B \to p\bar{p}K^*$ decays proceed predominantly through a $b \to s$ penguin loop diagram, which could be sensitive to new physics from heavy virtual particles in the loop. Large direct CP violation, $\sim$20%, is predicted using an effective-amplitude approach in the standard model [8]. From a pole model [9], it is expected that $\mathcal{B}(B^+ \to p\bar{p}K^{*+}) < \mathcal{B}(B^+ \to p\bar{p}K^+)$ due to the absence of some QCD penguin and electroweak penguin contributions in the $p\bar{p}K^{*+}$ mode, and that $\mathcal{B}(B^0 \to p\bar{p}K^{*0}) < \mathcal{B}(B^+ \to p\bar{p}K^{*+})$ due to the absence of a specific pole contribution and the external W emission diagram in the $p\bar{p}K^{*0}$ mode.

In this paper, we study the three-body charmless baryonic decays $B^0 \to p\bar{p}K^{*0}(K^{*0} \to K^+\pi^-)$ and $B^+ \to p\bar{p}K^{*+}(K^{*+} \to K^0_S\pi^+)$. The polarization of the K^* meson is determined, which provides information about the relative importance of penguin and external W-emission contributions [10]. The differential branching fractions as a function of the baryon-antibaryon mass and the polar angle distributions of the proton in the baryon-antibaryon system are also presented. The direct CP violation parameters of these two decays are also measured. We use a 492 fb^{-1} data sample, consisting of $535 \times 10^6 B\bar{B}$ pairs, collected

with the Belle detector at the KEKB asymmetric-energy e^+e^- (3.5 on 8 GeV) collider [12]. The Belle detector is a large-solid-angle magnetic spectrometer that consists of a silicon vertex detector (SVD), a 50-layer central drift chamber (CDC), an array of aerogel threshold Cherenkov counters (ACC), a barrel-like arrangement of time-of-flight (TOF) scintillation counters, and an electromagnetic calorimeter composed of CsI(Tl) crystals located inside a superconducting solenoid coil that provides a 1.5 T magnetic field. An iron flux-return located outside of the coil is instrumented to detect K^0_L mesons and to identify muons. The detector is described in detail elsewhere [13].

The event selection criteria for the primary charged tracks can be found in Ref. [14]. K^0_S candidates are reconstructed as $\pi^+\pi^-$ pairs with an invariant mass in the range 490 MeV/c^2 < $M_{\pi^+\pi^-}$ < 510 MeV/c^2. The candidate must have a displaced vertex and flight direction consistent with a K^0_S originating from the interaction point. We use the selected kaons and pions to form $K^{*+}(\to K^0_S\pi^+)$ and $K^{*0}(\to K^+\pi^-)$ candidates. Events with a K^* candidate mass between 0.6 GeV/c^2 and 1.2 GeV/c^2 are used for further analysis. Candidate B mesons are reconstructed in the $B^0 \to p\bar{p}K^{*0}$ and $B^+ \to p\bar{p}K^{*+}$ modes. We use two kinematic variables in the center-of-mass (c.m.) frame to identify the reconstructed B meson candidates: the beam energy constrained mass $M_{\text{bc}} = \sqrt{E^2_{\text{beam}} - p^2_B}$, and the energy difference $\Delta E = E_B - E_{\text{beam}}$, where E_{beam} is the beam energy, and p_B and E_B are the momentum and energy, respectively, of the reconstructed B meson. The candidate region is defined as 5.2 GeV/c^2 < M_{bc} <

5.3 GeV/c^2 and -0.1 GeV $< \Delta E < 0.3$ GeV. The lower bound in ΔE is chosen to exclude possible background from baryonic B decays with higher multiplicities. From a GEANT [15] based Monte Carlo (MC) simulation, the signal peaks in a signal box defined by the requirements 5.27 GeV/$c^2 < M_{bc} < 5.29$ GeV/c^2 and $|\Delta E| < 0.05$ GeV. To ensure the decay process is genuinely charmless, we apply charm vetoes. The regions 2.850 GeV/$c^2 < M_{p\bar{p}} < 3.128$ GeV/c^2 and 3.315 GeV/$c^2 < M_{p\bar{p}} < 3.735$ GeV/c^2 are excluded to remove background from modes with η_c, J/ψ and ψ', χ_{c0}, χ_{c1}, h_c mesons, respectively. The region 2.262 GeV/$c^2 < M_{pK_S^0}$, $M_{pK^-\pi^+} < 2.310$ GeV/c^2 is also excluded to remove a possible Λ_c^+ background. From a study of a charmless B decay MC sample, there are nonnegligible backgrounds in the candidate region due to $B^+ \to p\bar{p}K^+$ and $B^0 \to p\bar{p}K_S^0$. We remove the B candidates when their M_{bc} and ΔE values reconstructed for the $p\bar{p}K$ hypothesis are in the signal box.

After the above selection cuts, the background in the fit region arises dominantly from continuum $e^+e^- \to q\bar{q}$ ($q = u$, d, s, c) processes. We suppress the jetlike continuum background relative to the more spherical $B\bar{B}$ signal using a Fisher discriminant [16] that combines seven event shape variables, as described in Ref. [17]. Probability density functions (PDFs) for the Fisher discriminant and the cosine of the angle between the B flight direction and the beam direction in the Y(4S) rest frame are combined to form the signal (background) likelihood $\mathcal{L}_s$ ($\mathcal{L}_b$). The signal PDFs are determined using signal MC simulation; the background PDFs are obtained from the sideband data: 5.23 GeV/$c^2 < M_{bc} < 5.26$ GeV/c^2 and $|\Delta E| < 0.06$ GeV for the $p\bar{p}K^{*0}$ mode; 5.25 GeV/$c^2 < M_{bc} < 5.26$ GeV/c^2 and $|\Delta E| < 0.2$ GeV for the $p\bar{p}K^{*+}$ mode. The different selections for sideband regions of the two K^* modes ensure similar statistics to determine the background PDFs. We require the likelihood ratio $\mathcal{R} = \mathcal{L}_s/(\mathcal{L}_s + \mathcal{L}_b)$ to be greater than 0.7 for both decay modes. These selection criteria are determined by optimization of $n_s/\sqrt{n_s + n_b}$, where n_s and n_b denote the expected numbers of signal and background events in the signal box, respectively. We use the branching fractions from our previous measurements [4] in the calculation of n_s and use the number of sideband events to estimate n_b. If there are multiple B candidates in a single event, we select the one with the best χ^2 value from the vertex fit. The fractions of events that have multiple B candidates are 21% and 32% for the $p\bar{p}K^{*0}$ and $p\bar{p}K^{*+}$ modes, respectively.

We perform an unbinned extended likelihood fit that maximizes the likelihood function

$$L = \frac{e^{-(n_{K^*}+n_{K\pi}+n_{q\bar{q}})}}{N!} \prod_{i=1}^{N} (n_{K^*}P_{K^*} + n_{K\pi}P_{K\pi} + n_{q\bar{q}}P_{q\bar{q}})$$

to estimate the signal yield of $p\bar{p}K^*$ in the region

-0.1 GeV $< \Delta E < 0.3$ GeV, 5.2 GeV/$c^2 < M_{bc} <$ 5.3 GeV/c^2 and 0.6 GeV/$c^2 < M_{K\pi} < 1.2$ GeV/c^2; here N is the number of events in the fit, and n_{K^*}, $n_{K\pi}$ and $n_{q\bar{q}}$ are fit parameters representing the yields of $B \to p\bar{p}K^*$, $B \to p\bar{p}K\pi$ and continuum background, respectively. Each PDF is the product of shapes in M_{bc}, ΔE and $M_{K\pi}$, which are assumed to be uncorrelated, e.g., for the ith event, $P_{p\bar{p}K^*} = P_{M_{bc}}(M_{bc_i}) \times P_{\Delta E}(\Delta E_i) \times P_{K\pi}(M_{K\pi_i})$.

For the PDFs of $p\bar{p}K^{*0}$, $p\bar{p}K^{*+}$ and $p\bar{p}K\pi$ decay modes, we use a Gaussian function to represent $P_{M_{bc}}$ and a double Gaussian for $P_{\Delta E}$ with parameters determined by MC signal events. Moreover, we use a p-wave Breit-Wigner function [18] to parameterize the $P_{M_{K\pi}}$ distribution for $p\bar{p}K^{*0}$ and $p\bar{p}K^{*+}$ and use a function obtained by the LASS collaboration [19] for $p\bar{p}K\pi$. The parameters of these PDFs have been modified to account for the differences between data and MC calculations using control samples of $J/\psi K^{*0}$ and $J/\psi K^{*+}$ with $J/\psi \to p\bar{p}$. The modifications related to the mass peaks are all less than 1 MeV/c^2. The ΔE distribution has a ~ -3 MeV shift while the modification for its width is ~ 1 MeV. For the continuum background PDFs, we use a parameterization that was first employed by the ARGUS collaboration [20], $f(M_{bc}) \propto M_{bc}\sqrt{1-x^2} \times e^{-\xi(1-x^2)}$, to model the $P_{M_{bc}}$ with x given by M_{bc}/E_{beam} and where ξ is a fit parameter. The $P_{\Delta E}$ distribution
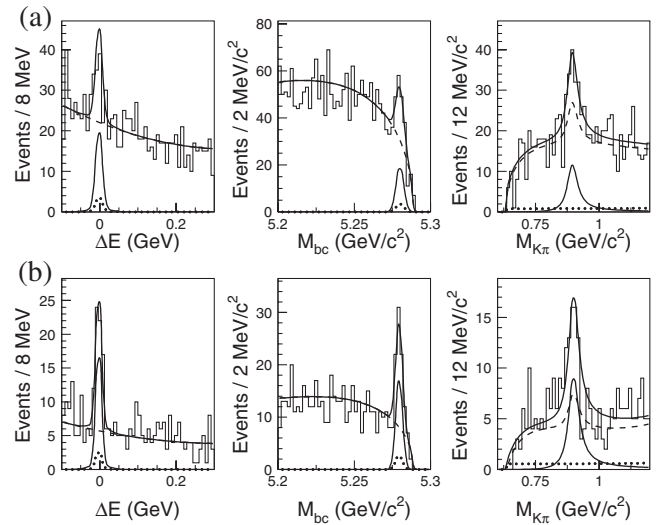

FIG. 1. Distributions of ΔE (with 5.27 GeV/$c^2 < M_{bc} <$ 5.29 GeV/c^2 and 0.812 GeV/$c^2 < M_{K\pi} < 0.972$ GeV/c^2), M_{bc} (with $|\Delta E| < 0.05$ GeV and 0.812 GeV/$c^2 < M_{K\pi} <$ 0.972 GeV/c^2) and $M_{K\pi}$ (with $|\Delta E| < 0.05$ GeV and 5.27 GeV/$c^2 < M_{bc} < 5.29$ GeV/c^2), respectively, with proton-antiproton pair mass less than 2.85 GeV/c^2 for (a) $p\bar{p}K^{*0}$ and (b) $p\bar{p}K^{*+}$ modes. The solid curves, solid peaks, dotted curves and dashed curves represent the combined fit result, fitted $B \to p\bar{p}K^*$ signal, $B \to p\bar{p}K\pi$ signal and fitted background, respectively. The areas of dotted curves are about 15% of those of the solid peaks.

TABLE I. Signal yields and branching fractions $\mathcal{B}$ (10^{-6}) in different $M_{p\bar{p}}$ regions for $B^0 \to p\bar{p}K^{*0}$(left) and $B^+ \to p\bar{p}K^{*+}$ (right).

$M_{p\bar{p}}$ (GeV)	$p\bar{p}K^{*0}$ Yield	$p\bar{p}K^{*0}$ $\mathcal{B}$ (10^{-6})	$p\bar{p}K^{*+}$ Yield	$p\bar{p}K^{*+}$ $\mathcal{B}$ (10^{-6})
<2.0	$21.4^{+8.0}_{-7.1}$	$0.30^{+0.11}_{-0.10}$	$9.0^{+4.4}_{-3.7}$	$0.43^{+0.21}_{-0.18}$
2.0–2.2	$21.5^{+8.4}_{-7.5}$	$0.31^{+0.12}_{-0.11}$	$25.1^{+7.1}_{-6.3}$	$1.28^{+0.36}_{-0.32}$
2.2–2.4	$15.7^{+6.4}_{-5.6}$	$0.26^{+0.10}_{-0.09}$	$6.4^{+5.4}_{-4.5}$	$0.37^{+0.31}_{-0.26}$
2.4–2.6	$12.3^{+6.2}_{-5.4}$	$0.22^{+0.11}_{-0.10}$	$4.5^{+3.3}_{-2.5}$	$0.30^{+0.22}_{-0.17}$
2.6–2.85	$1.2^{+4.9}_{-3.9}$	$0.02^{+0.09}_{-0.07}$	$9.6^{+4.8}_{-3.9}$	$0.62^{+0.31}_{-0.25}$
2.85–3.128(veto)	$224.2^{+18.2}_{-17.6}$	$4.12^{+0.34}_{-0.32}$	$55.7^{+9.8}_{-9.0}$	$3.66^{+0.65}_{-0.59}$
3.128–3.315	$2.6^{+4.7}_{-3.5}$	$0.05^{+0.09}_{-0.06}$	$1.5^{+2.1}_{-1.5}$	$0.11^{+0.15}_{-0.11}$
3.315–3.735(veto)	$11.9^{+6.6}_{-5.6}$	$0.24^{+0.13}_{-0.11}$	$7.1^{+4.8}_{-4.1}$	$0.58^{+0.40}_{-0.34}$
>3.735	$0.7^{+5.5}_{-4.4}$	$0.02^{+0.14}_{-0.11}$	$2.5^{+2.9}_{-2.0}$	$0.27^{+0.31}_{-0.22}$
Charmless	$75.4^{+17.1}_{-14.7}$	$1.18^{+0.29}_{-0.25}$	$58.7^{+12.1}_{-10.1}$	$3.38^{+0.73}_{-0.60}$

is modeled by a normalized second-order polynomial whose coefficients are fit parameters. The PDF $P_{M_{K\pi}}$ is modeled by a p-wave function and a threshold function, $P_{M_{K\pi}} = rP_{p-\text{wave}} + (1-r)P_{\text{threshold}}$ and $P_{\text{threshold}} \propto (M_{K\pi} - M_K - M_\pi)^s e^{[c_1(M_{K\pi}-M_K-M_\pi)+c_2(M_{K\pi}-M_K-M_\pi)^2]}$, where r, s, c_1, and c_2 are fit parameters. Figure 1 shows the fits used to obtain the $B \to p\bar{p}K^*$ yields in the proton-antiproton mass region below 2.85 GeV/c^2, which we refer to as the threshold-mass-enhanced region. The signal yields are $70.1^{+14.8}_{-13.9}$ and $54.2^{+10.9}_{-10.1}$ with statistical significances of 7.2 and 8.8 standard deviations for the $p\bar{p}K^{*0}$ and $p\bar{p}K^{*+}$ modes, respectively. The significance is defined as $\sqrt{-2\ln(L_0/L_{\max})}$, where L_0 and $L_{\max}$ are the likelihood values returned by the fit with the signal yield fixed to zero and at its best fit value.

We determine the angular distribution of the K^* meson in the region $M_{p\bar{p}} < 2.85$ GeV/c^2 using likelihood fits to

obtain signal yields in bins of $\cos\theta_K$, where θ_K is the polar angle of the K meson in the K^* helicity frame. The theoretical PDF for the K^* meson has the form $3/2 \cos^2\theta_K$ for a pure helicity zero state and $3/4 \sin^2\theta_K$ for a pure helicity one (± 1) state. We use MC simulation to obtain the efficiency function and convolve it with the theoretical forms in order to obtain the final PDFs for different helicity states. The signal yields in bins of $\cos\theta_K$ are then fitted with the above two different PDFs where the fraction of the helicity zero state is floated in the fit and the total yield is fixed to the experimental result. The B yield distributions in bins of $\cos\theta_K$ with the corresponding fit curves are shown in Fig. 2. We find that the K^{*0} meson has a fraction of $(101 \pm 13 \pm 3)\%$ in the helicity zero state and the K^{*+} meson has a $(32 \pm 17 \pm 9)\%$ fraction in the helicity zero state. It is interesting to note that the helicity zero amplitude is expected to be dominant in the $b \to s$ penguin transition due to the $(V\text{-}A)$ nature of the weak interaction and helicity conservation in the strong interaction [10]. The systematic uncertainty is obtained from the $B \to J/\psi K^*$, $J/\psi \to \mu^+\mu^-$ control sample. We compare our measured K^* polarization in the helicity zero state with the PDG value [11]. The difference is added in quadrature with the PDG error and the fit error to extract the final systematic uncertainty. These uncertainties are 0.03 and 0.09 for the $p\bar{p}K^{*0}$ and $p\bar{p}K^{*+}$ modes, respectively.

Since the detection efficiency depends on $M_{p\bar{p}}$, we determine the $B \to p\bar{p}K^*$ yields in bins of $M_{p\bar{p}}$. We generate a large phase-space MC sample in order to estimate the efficiencies properly where the subdecay branching fractions of K^* to corresponding final states are included. The $K\pi$ angular distribution is fixed by the measured K^* polarization for all $M_{p\bar{p}}$ bins. The partial branching fractions are obtained by correcting the fitted B yields for the mass-dependent efficiencies. The differential branching fractions as a function of the proton-antiproton mass for both $p\bar{p}K^{*0}$ and $p\bar{p}K^{*+}$ modes are shown in Fig. 3, and the measured branching fractions for different $M_{p\bar{p}}$ bins are
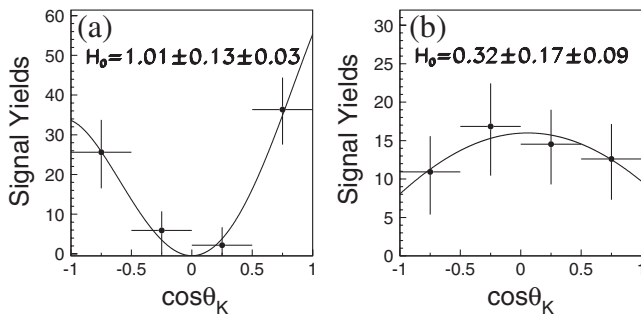

FIG. 2. B yield distributions as functions of $\cos\theta_K$ with fit curves overlaid for (a) the $p\bar{p}K^{*0}$ mode and (b) the $p\bar{p}K^{*+}$ mode. The fraction of the signal in the helicity zero state is the fit parameter and is denoted by H_0. The asymmetries in the fit curves are due to detection efficiencies. The underlying theoretical distributions are symmetric.
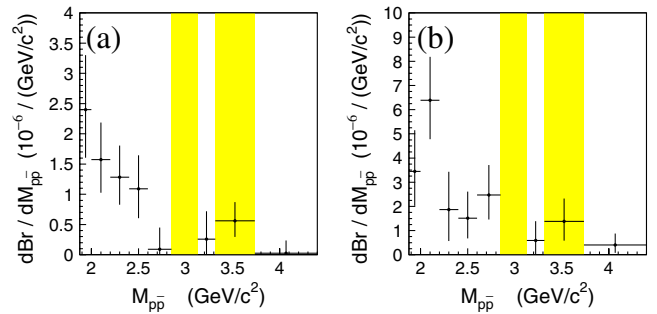

FIG. 3 (color online). Differential branching fractions for (a) the $p\bar{p}K^{*0}$ and (b) the $p\bar{p}K^{*+}$ modes as a function of proton-antiproton invariant mass. Note that the two shaded mass bins contain charmonium events and are excluded from the charmless signal yields. The data points for the 2.85 GeV/$c^2 < M_{p\bar{p}} < 3.128$ GeV/c^2 mass region are off-scale.

listed in Table I. Applying 3.075 GeV/$c^2 < M_{p\bar{p}} <$ 3.117 GeV/c^2 for J/ψ selection, we find good agreement, within 1σ, between our branching fraction measurements and the PDG values [11]. In contrast to Ref. [7], we find that a threshold enhancement is present for the $B^0 \rightarrow p\bar{p}K^{*0}$ decay. With the charmonium regions excluded, we sum these partial branching fractions to obtain: $\mathcal{B}(B^0 \rightarrow p\bar{p}K^{*0}) = (1.18^{+0.29}_{-0.25} \pm 0.11) \times 10^{-6}$ and $\mathcal{B}(B^+ \rightarrow p\bar{p}K^{*+}) = (3.38^{+0.73}_{-0.60} \pm 0.39) \times 10^{-6}$. As a by-product of our analysis, we also use the $B^+ \rightarrow p\bar{p}K^+$ and $B^0 \rightarrow p\bar{p}K^0_S$ signals to estimate the corresponding branching fractions in different $M_{p\bar{p}}$ bins. The total charmless branching fraction $\mathcal{B}(B^+ \rightarrow p\bar{p}K^+)$ is $(5.36^{+0.23}_{-0.22}) \times 10^{-6}$, which agrees well with our latest results, $(5.54^{+0.27}_{-0.25} \pm 0.36) \times 10^{-6}$ [14]. The measured value of $\mathcal{B}(B^0 \rightarrow p\bar{p}K^0)$ is $(2.51^{+0.35}_{-0.29} \pm 0.21) \times 10^{-6}$. This result also supersedes our previous measurement [4]. With improved experimental accuracy, the following relationships $\mathcal{B}(B^+ \rightarrow p\bar{p}K^+) > \mathcal{B}(B^+ \rightarrow p\bar{p}K^{*+})$ and $\mathcal{B}(B^+ \rightarrow p\bar{p}K^{*+}) > \mathcal{B}(B^0 \rightarrow p\bar{p}K^{*0})$ are established. These inequalities agree with the pole model predictions [9], but the measured $\mathcal{B}(B^0 \rightarrow p\bar{p}K^{*0})$ is about a factor of 20 larger than predicted. This may indicate that the relative weights of different pole contributions in Ref. [9] are incorrect.

Systematic uncertainties are determined using high-statistics control data samples. For proton identification, we use a $\Lambda \rightarrow p\pi^-$ sample, while for K/π identification we use a $D^{*+} \rightarrow D^0\pi^+$, $D^0 \rightarrow K^-\pi^+$ sample. Note that the average efficiency difference for PID between data and MC calculations has been corrected to obtain the final branching fraction measurements. The corrections are about 11.5% and 11.7% for the $p\bar{p}K^{*0}$ and $p\bar{p}K^{*+}$ modes, respectively. The uncertainties associated with the PID corrections are estimated to be 4% for two protons and 1% for one kaon or pion. The tracking uncertainty is determined with fully and partially reconstructed D^* samples. It is about 1% per charged track. The uncertainty in K^0_S reconstruction is determined to be 4% from a sample of $D^- \rightarrow K^0_S\pi^-$ events. The $\mathcal{R}$ continuum suppression uncertainty of 2.3% is estimated from control samples with similar final states, $B \rightarrow J/\psi K^*$ with $J/\psi \rightarrow \mu^+\mu^-$. The uncertainties in the best B candidate selection are estimated to be 2.0% and 3.5% for the $p\bar{p}K^{*0}$ and $p\bar{p}K^{*+}$ modes, respectively, by taking a difference in the branching fractions with and without the best candidate selection. A systematic uncertainty of 5.2% in the fit yield is determined by varying the parameters (or changing the functional forms) of the signal and background PDFs. The MC statistical uncertainty is less than 3%. The efficiency error caused by the K^* polarization modeling is estimated to be 2.4% and 4.0% for the $p\bar{p}K^{*0}$ and $p\bar{p}K^{*+}$ modes, respectively, by changing the polarization value by $\pm 1\sigma$. The error on the number of $B\bar{B}$ pairs is 1.3%, where we assume that the branching fractions of $\Upsilon(4S)$ to neutral and charged $B\bar{B}$ pairs are equal. We first sum the correlated errors linearly and then combine them with the uncorrelated ones in quadrature. The total systematic uncertainties are 9.7% and 11.6% for the $p\bar{p}K^{*0}$ and $p\bar{p}K^{*+}$ modes, respectively.

We study the proton angular distribution in the proton-antiproton helicity frame with $M_{p\bar{p}} < 2.85$ GeV/c^2. The angle θ_p is defined as the angle between the proton direction and the positive strangeness K^* (i.e., K^{*-} or $\bar{K}^{*0}$) direction in the proton-antiproton pair rest frame. The $\cos\theta_p$ distributions, shown in Fig. 4, do not have a prominent peaking feature toward $\cos\theta_p \sim 1$, which was first observed in the decay $B^+ \rightarrow p\bar{p}K^+$ [21]. However, current statistics are inadequate to draw any definitive conclusions about $B \rightarrow p\bar{p}K^*$.

To examine the prediction [8] that direct CP violation in $B^+ \rightarrow p\bar{p}K^{*+}$ can be as large as $\sim 20\%$, we define the charge asymmetry A_{ch} as $(N_b - N_{\bar{b}})/(N_b + N_{\bar{b}})$ for the $p\bar{p}K^{*0}$ and $p\bar{p}K^{*+}$ modes, where N and b stand for the efficiency corrected B yield and quark flavor, respectively. The results are $-0.08 \pm 0.20 \pm 0.02$ and $-0.01 \pm 0.19 \pm 0.02$ for the $p\bar{p}K^{*0}$ and $p\bar{p}K^{*+}$ modes, respectively. The systematic uncertainty is estimated from the measured charge asymmetry for the sideband data.

In summary, using $535 \times 10^6 B\bar{B}$ events and applying charmonium vetoes, we observe the $B^0 \rightarrow p\bar{p}K^{*0}$ decay with a branching fraction of $(1.18^{+0.29}_{-0.25}(\mathrm{stat}) \pm 0.11(\mathrm{syst})) \times 10^{-6}$. The signal yield is $70.1^{+14.8}_{-13.9}$ with a significance of 7.2 standard deviations in the $M_{p\bar{p}} < 2.85$ GeV/c^2 mass region. The K^{*0} meson is found to be $(101 \pm 13 \pm 3)\%$ in the helicity zero state, compared to $(32 \pm 17 \pm 9)\%$ for the K^{*+} meson. The smaller K^{*+} polarization in the $p\bar{p}K^{*+}$ decay may be attributed to an additional contribution from external W emission. We also observe a low mass $p\bar{p}$ enhancement near threshold for the $p\bar{p}K^{*0}$ mode. The direct CP asymmetries for $p\bar{p}K^{*0}$ and $p\bar{p}K^{*+}$ are measured to be $-0.08 \pm 0.20 \pm 0.02$ and $-0.01 \pm 0.19 \pm 0.02$, respectively. With improved experimental accuracy, the relationships $\mathcal{B}(B^+ \rightarrow p\bar{p}K^+) > \mathcal{B}(B^+ \rightarrow p\bar{p}K^{*+})$ and $\mathcal{B}(B^+ \rightarrow p\bar{p}K^{*+}) > \mathcal{B}(B^0 \rightarrow p\bar{p}K^{*0})$ are established.
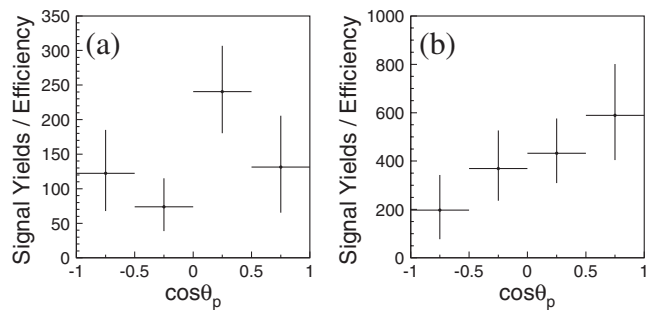

FIG. 4. Distributions of efficiency corrected signal yields *vs.* $\cos\theta_p$ in the proton-antiproton system with $M_{p\bar{p}} < 2.85$ GeV/c^2 for (a) $B^0 \rightarrow p\bar{p}K^{*0}$ and (b) $B^+ \rightarrow p\bar{p}K^{*+}$.

[1] K. Abe *et al.* (Belle Collaboration), Phys. Rev. Lett. **88**, 181803 (2002).

[2] Throughout this Letter, inclusion of charge-conjugate mode is always implied unless otherwise stated.

[3] M. Z. Wang *et al.* (Belle Collaboration), Phys. Rev. Lett. **90**, 201802 (2003).

[4] M. Z. Wang *et al.* (Belle Collaboration), Phys. Rev. Lett. **92**, 131801 (2004).

[5] Y. J. Lee *et al.* (Belle Collaboration), Phys. Rev. Lett. **93**, 211801 (2004).

[6] Y. J. Lee *et al.* (Belle Collaboration), Phys. Rev. Lett. **95**, 061802 (2005).

[7] B. Aubert *et al.* (*BABAR* Collaboration), Phys. Rev. D **76**, 092004 (2007).

[8] C. Q. Geng, Y. K. Hsiao, and J. N. Ng, Phys. Rev. Lett. **98**, 011801 (2007); C. Q. Geng, Y. K. Hsiao, and J. N. Ng, Phys. Rev. D **75**, 094013 (2007).

[9] H. Y. Cheng and K. C. Yang, Phys. Rev. D **66**, 014020 (2002).

[10] For a review article and references therein, see [11], p. 833.

[11] W.-M. Yao *et al.* (Particle Data Group), J. Phys. G **33**, 1 (2006).

[12] S. Kurokawa and E. Kikutani, Nucl. Instrum. Methods Phys. Res., Sect. A **499**, 1 (2003), and other papers included in this volume.

[13] A. Abashian *et al.* (Belle Collaboration), Nucl. Instrum. Methods Phys. Res., Sect. A **479**, 117 (2002).

[14] J.-T. Wei *et al.* (Belle Collaboration), Phys. Lett. B **659**, 80 (2008).

[15] R. Brun *et al.*, GEANT 3.21, CERN Report No. DD/EE/ 84-1, 1987.

[16] R. A. Fisher, Annals of Eugenics **7**, 179 (1936).

[17] K. Abe *et al.* (Belle Collaboration), Phys. Lett. B **517**, 309 (2001).

[18] J. Zhang *et al.* (Belle Collaboration), Phys. Rev. Lett. **95**, 141801 (2005).

[19] D. Aston *et al.* (LASS Collaboration), Nucl. Phys. **B296**, 493 (1988).

[20] H. Albrecht *et al.* (ARGUS Collaboration), Phys. Lett. B **241**, 278 (1990); **254**, 288 (1991).

[21] M. Z. Wang *et al.* (Belle Collaboration), Phys. Lett. B **617**, 141 (2005).